Review

Quantum Dot Sensitized Solar Cell: Photoanodes, Counter Electrodes, and Electrolytes

Nguyen Thi Kim Chung [1], Phat Tan Nguyen [2], Ha Thanh Tung [3,*] and Dang Huu Phuc [4,5,*]

1 Thu Dau Mot University, Number 6, Tran Van on Street, Phu Hoa Ward, Thu Dau Mot 55000, Vietnam; chungntk@tdmu.edu.vn
2 Department of Physics, Ho Chi Minh City University of Education, Ho Chi Minh City 70250, Vietnam; phatnt@hcmup.edu.vn
3 Faculty of Physics, Dong Thap University, Cao Lanh City 870000, Vietnam
4 Laboratory of Applied Physics, Advanced Institute of Materials Science, Ton Duc Thang University, Ho Chi Minh City 70880, Vietnam
5 Faculty of Applied Sciences, Ton Duc Thang University, Ho Chi Minh City 70880, Vietnam
* Correspondence: httung@dthu.edu.vn (H.T.T.); danghuuphuc@tdtu.edu.vn (D.H.P.)

Abstract: In this study, we provide the reader with an overview of quantum dot application in solar cells to replace dye molecules, where the quantum dots play a key role in photon absorption and excited charge generation in the device. The brief shows the types of quantum dot sensitized solar cells and presents the obtained results of them for each type of cell, and provides the advantages and disadvantages. Lastly, methods are proposed to improve the efficiency performance in the next researching.

Keywords: optical; electrical; photovoltaic; photoanodes; counter electrodes; electrolytes

1. Introduction

Solar cells have grown very rapidly over the past few decades, which are divided into three generations: the first generation is a monocrystalline and polycrystalline Si solar cell with an efficiency of 26.7% [1] and 21.9% [2], respectively. The 2nd generation solar cells are a thin film such as CdTe [3], amorphous Si [4], the cost is lower than the 1st generation, and the efficiency is 21.7% [5]. The 3rd generation solar cells include dye sensitized solar cells (DSSCs), quantum dot sensitized solar cells (QDSSCs), perovskite cells with much lower cost than the 1st and the 2nd generation, and photoelectric conversion efficiency of over 40% according to the theoretical calculation. The highest yield obtained for DSSCs 11.9% lower than that of perovskite solar cells (19.7%) [6]. This shows the huge potential of the perovskite solar cell, it reaches an efficiency of 25.2% by 2020 [7], and it is predicted to reach 28% in the future. In addition to perovskite cells, QDSSCs are predicted to reach more than 40% efficiency according to theoretical calculations, this is also very potentially a 3rd generation solar cell.

One of the main reasons for the growing interest in quantum dots is their use in cheap solar cells, which have the possibility to increase the thermodynamic conversion efficiency above the Shockley–Queisser limit [8]. The thermodynamic limit of the light to electric power conversion efficiency, also known as Shockley–Queisser limit, originates from the fact that photons with energies below the band gap energy are not absorbed, while photons with energies above the band gap energy release the additional energy ($E_{photon} - E_{gap}$) mostly as heat. Third generation solar cells aim for conversion efficiencies beyond the Shockley–Queisser limit through advanced photovoltaic concepts such as multijunction cells, optical up and down converters, and multiple carrier generation by impact ionization. Their development has been based on different p–n junctions and the use of quantum dots (QDs) to replace dyes. Performance above 40% has been obtained [9].

Now the focus is on the next generation solar cells with high efficiency at an economically viable cost [10,11]. QDs are drawing great attention as a material for the next generation solar cells due to high absorption coefficient, tunable band gap, and multiple exciton generation (MEG) effect [12,13]. Therefore, QDs have been used in dye-sensitized solar cells (DSSCs) as the photosensitizer instead of organic dyes to form quantum dot sensitized solar cells (QDSSCs) [14–16]. The typical structure of the QDSSCs is similar to that of the DSSCs, which consists of mesoporous photo anode (TiO_2 film), sensitizer (QDs), electrolyte (polysulfide), and the counter electrode [17–20]. During operation, photons are captured by QDs, yielding electron–hole pairs that are rapidly separated into electrons and holes at the interface between the nanocrystalline TiO_2 and the QDs. The electrons inject into the TiO_2 film and the holes are released by redox couples in the liquid polysulfide electrolyte [17,20,21].

Improving the power conversion efficiency (η) of QDSSCs has always been an overarching concern for all scientists. One of the approaches has been focused on constructing and fabricating nanostructural oxides, such as TiO_2 [22], ZnO [23,24], and SnO_2 [25] to harvest more amounts of QDs. On the other hand, many efforts have been concentrated on designing and synthesizing QDs to get high photoelectric performance [26–28].

In recent years, researchers have discovered the QDs, which can create the high performance of solar cells [29]. QDs can be changed in particle size, leading to a change in the absorption spectrum [30]. Controlling QDs size, we can change their absorption spectrum. Furthermore, in association with biological molecules, QDs can transfer charge faster while reducing losses and helping the passivated surface (reduced defect states) of them. In 1990, Vogel and his colleagues have used CdS QDs with the Pt cathode [31]. However, this is a new direction in QDSSCs research. Since then, there have been a large number of studies such as different QDs replacement, TiO_2 semiconductor materials, electrolyte, and counter electrodes to enhance the photovoltaic performance [32–34]. Lee and his colleagues studied CdSe and CdTe QDs using the Pt counter electrode with an efficiency of under 1% [35]. One year later (2008), they went on investigating CdS and CdSe QDs and improved the performance efficiency to 1.2% with the use of polysulfide electrolyte [32]. Meanwhile, Lopez-Luke et al., Mora–Sero et al., Shen et al., and Tachibana et al. [36–39] synthesized CdS and CdSe QDs with the Pt counter electrode, but in different electrolyte systems (Na_2S, NaOH + Na_2S+S) and obtained a better performance efficiency of 2.2%. From 2009 to 2012, various QDSSCs were studied. Cheng et al. [40] examined CdS and CdSe cosensitized TiO_2 nanowires and nanorods by using the Na_2S+Na_2SO_3 electrolyte and obtained a high efficiency of 2.41%.

Recently, a few research showed that some doping ions in the sulfide QDs, such as Hg^{2+} into PbS [41], and Mn^{2+} into CdS [42], could increase the current density and efficiency of the solar cells. Compared with CdS and PbS QDs, CdSe are more attractive owing to its high potential for light harvesting in the visible light region [43,44]. The efficiency of CdSe QDs sensitized solar cells is much higher than that of the sulfide QDs sensitized solar cells [45–49]. Therefore, doping metal ions into CdSe QDs is considered a useful way for designing high efficiency solar cells [50,51].

In this study, a review on QDSSCs based on photoanodes with single quantum dot, with binding agents, with passive surfactant, with multilayer QDs, and with doped QDs, different counter electrodes, and different electrolytes are briefly provided.

2. Quantum Dot Sensitized Solar Cells (QDSSCs) Based on Single Quantum Dots (QDs) Photoanode

2.1. A Review on QDSSCs Based on Single QDs

Single QDs are individual QDs synthesized by several methods such as colloidal QD, chemical bath deposition (CBD), successive ionic layer absorption and reaction (SILAR), etc. Those QDs are assembled on the surface of metal oxides, which have large electronic bandgaps such as TiO_2, ZnO, SnO_2, etc. Both QDs and metal oxide layers are put on top of fluorine doped tin oxide (FTO) substrates to form a complete photoanode, which is illustrated in Figure 1. Thus far, there are many QDs that have been attractive globally, for example, PbS [52,53], $CuInS_2$ [54], $AgInSe_2$ [55], PbSe [56], Ag_2Se [57], CdS [58], CdSe [59],

CdTe [60], etc. Among them, CdS, CdSe, and CdTe QDs are prominent candidates because of their high stability in fabricated QDSSCs [61] and achieving the highest photoelectric conversion efficiency (PCE) as illustrated in Table 1.
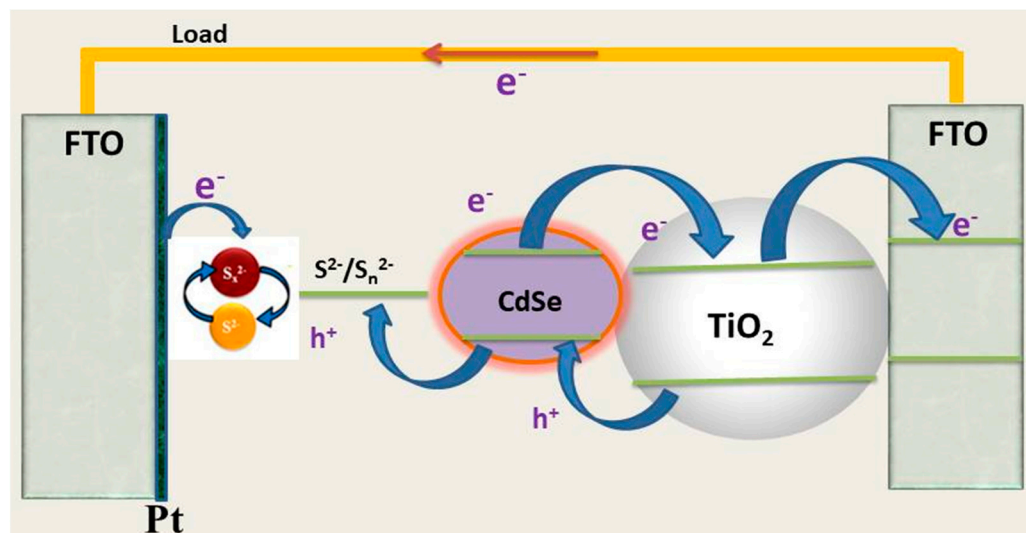

Figure 1. Schematic of a QDSSC's structure with a single QDs CdSe photoanode.

Table 1. Review of the same field publications.

Metal Oxide Layer	QDs	Counter Electrode	Electrolyte	Synthesis Method	FF (%)	PCE (%)	Ref
TiO_2	CdS	Pt	$KCl+Na_2S$	SILAR	-	-	[61]
TiO_2	CdSe	Pt	$[Fe(CN)_6]^{3-/4-}$	CBD	-	-	[62]
TiO_2	CdSe	Pt	$Na_2S+Na_2SO_4$	CBD	-	-	[63]
TiO_2	CdS	Pt	Na_2SO_3	CBD	-	-	[64]
TiO_2	CdSe	Pt	Polysulfide	CBD	59	1.03	[65]
TiO_2	CdSe	Pt	Na_2S	CBD	40	0.7	[66]
TiO_2	CdSe	Pt	Na_2S	CBD	27.7	0.84	[67]
TiO_2	CdSe	Pt	$Na_2S+S+NaOH$	CBD	43	0.4	[68]
TiO_2	CdS	Pt	$LiI+I_2+DMPII+TPB$	CBD	70	0.3	[69]
TiO_2	CdSe	Pt	$LiI+I_2+HMII+TPB$	CBD, Linker	56.3	1.19	[70]
TiO_2	CdS/CdSe	Pt	Na_2S+S	CBD	41.5	1.42	[71]
TiO_2	CdS	Pt	$KCl+Na_2S$	SILAR	-	-	[72]
TiO_2	CdS/CdSe	Pt	$Na_2S+S+KCl$	SILAR	36	1.14	[73]
TiO_2	CdS/ZnSe	Pt	Thiourea	CBD, Linker	58	0.86	[74]
TiO_2	CdS/CdSe	Pt	$Na_2S+S+KCl$	CBD	37	1.33	[75]
TiO_2	CdS/CdSe/ZnS	CuS, CoS	Polysulfide	SILAR	35	2.7	[76]
TiO_2	CdS/ZnS	Pt	Sulfide	SILAR	46	1.72	[77]
TiO_2/ZnS	CdS/CdSe	Cu_2S	Na_2S+S	SILAR	66	4.21	[78]
TiO_2	CdS/CuInS$_2$	Carbon	Na_2S+S	Colloid	37	1.47	[79]
TiO_2	CdS/JK24	Pt	Na_2S+S	Colloid	38.2	1.18	[80]
Graphene-TiO_2	CdS	Pt	Na_2S+S	Colloid	41	1.31	[81]
TiO_2	CdS/CdSe	Pt	$Na_2S+S+KCl$	SILAR	36	1.14	[73]
TiO_2	CdS/ZnSe	Pt	Thiourea	CBD, Linker	58	0.86	[74]

When a photon is absorbed, an excited electron is generated in the conduction band of a single QDs and transferred to the metal oxide layer to form a close electronic circuit. Several PCE of QDSSCs based on single QDs are shown in Table 1, whose efficiencies are relatively small, specifically, 1.31% and 1.03% [62], the highest PCE for CdS and CdSe QDs, respectively. These results are due to the absorption spectra of CdS and CdSe QDs being limited to 450 and 550 nm wavelength, respectively. This leads to the strong absorption of QDs with photons whose wavelengths are shorter than 550 nm. Otherwise, QDs are transparent to photons having wavelengths longer than 550 nm. Due to the restriction of QDs' absorption spectra, the number of electrons produced after photo excitation is limited and greatly lost due to recombination centers (the material is imperfectly fabricated) resulting in low current density and clearly small PCE.

2.2. The Causes of Low QDSSCs' PCE and Solutions

Based on the references and obtained results, there are some main reasons for the reduction of QDSSCs' PCE, which are:

a.   Low fill factor

The fill factor (FF) is defined from the current density–voltage (J–V) characteristic measurement. FF depends on the value of open circuit potential, resistance of series-connected components, and recombination processes in the QDSSCs, which relate to the fabricated materials. Low FF may be caused by the small open circuit potential, which strongly depends on the photoanode, and excessive recombination in QDSSCs. Moreover, FF is also affected by series resistors and parallel resistors of QDSSCs. To achieve higher PCE and reduce recombination in QDSSCs, it is required to have smaller series resistance R_S and larger parallel resistance R_{SH}. From Table 1, R_S values of QDSSCs based on CdSe QDs are relatively large, in the range of 27.4–732 Ω. This obstructs the electrons moving through the contact layers. Similarly, relatively small R_{SH} values, which can be seen in Table 2, tend to reduce the performance of QDSSCs.

Table 2. The resistance values of QDSSCs as calculated by physical approach.

| QDSSCs	R_D (Ω)	R_d (Ω)	R_S (Ω)	R_{SH} (Ω)	PCE η (%)
1-h soaked TiO$_2$/CdSe	1230.0	498.0	732.0	239.0	0.020
10-h soaked TiO$_2$/CdSe	538.2	382.0	156.2	588.1	0.046
18-h soaked TiO$_2$/CdSe	157.3	83.1	74.2	2027.0	0.184
20-h soaked TiO$_2$/CdSe	60.8	33.2	27.4	5396.0	0.575
24-h soaked TiO$_2$/CdSe	136.5	80.0	56.5	2130.0	0.150

b.   Impaired electrolyte

To investigate the factors that can cause a reduction in QDSSCs' PCE, the reduced absorption ability of the electrolyte after photoanode immersion is studied. According to Kamat et al., the electrolyte is in direct contact with the TiO$_2$/CdSe membrane, so, in operation, CdSe QDs react with the electrolyte and generate byproducts, which impair both the electrolyte and CdSe QDs. Those reactions are described by the following equations:
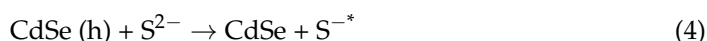
- A dynamic balance is existed in the S^{2-}/S_n^{2-} aqueous electrolyte:

$$S^{2-} + H_2O \leftrightarrow HS^- + OH^- \tag{1}$$

- Electron–hole pairs are generated after CdSe QDS are photoexcited by possibly the following equations:

$$CdSe + h\nu \rightarrow CdSe\ (e + h) \rightarrow CdSe + h\nu' \tag{2}$$

$$CdSe\ (e + h) + TiO_2 \rightarrow CdSe\ (h) + TiO_2\ (e) \tag{3}$$
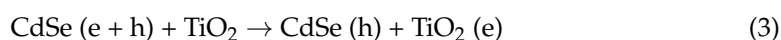
- Reaction at the CdSe/electrolyte interface:

$$CdSe\ (h) + S^{2-} \rightarrow CdSe + S^{-*} \tag{4}$$

- The S^{2-}/S_n^{2-} strongly obstructs the hole movement from CdSe QDs into the electrolyte [27] as described in Equation (4) and S^{-*} is in an excited ion.

As can be seen in Figure 2, the absorption of the electrolyte was dramatically decreased after 2 days of immersion. This proves the large influence of the electronic exchange reactions between CdSe QDs and the electrolyte, as generated byproducts from Equations (1)–(4) impaired the electrolyte absorbance and reduced the QDSSCs' PCE.
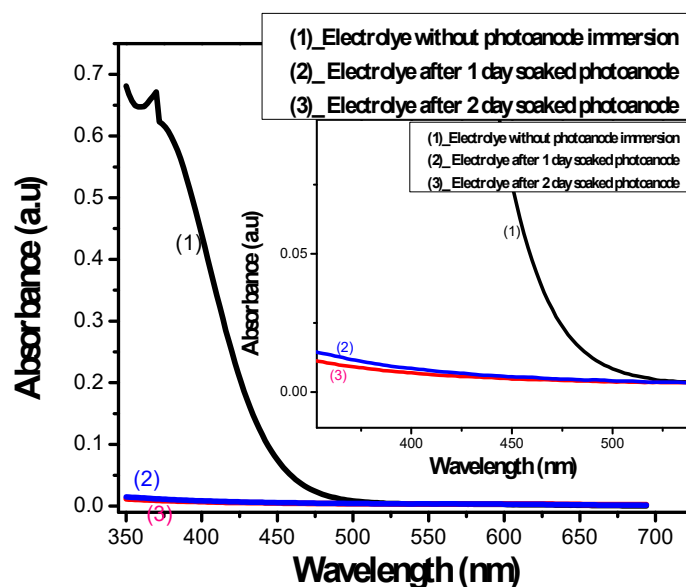
Figure 2. The absorption spectrum of polysulfide electrolyte before and at specific times after photoanode immersion.

c.   Strong recombination processes

A typical structure of QDSSCs includes the photoanode, counter electrode, and polysulfide electrolyte. Under the light condition, the operated processes happening inside QDSSCs are shown in Figure 3. These processes are indicated by arrows. When the photoanode surface is illuminated, exciton generation and electron–hole recombination are exhibiting simultaneously inside CdSe QDs (1). Free electrons in the conduction band of CdSe QDs are easily transferred to the TiO_2 conduction band (2). Those electrons, however, may be trapped in surface states due to CdSe QDs imperfection (3) and diffused into the electrolyte afterward (4), or recombined with holes inside CdSe QDs. The recombination of free electrons in the conduction band (CB) with CdSe QDs surface state and the recombination of electrons in the electrolyte and holes in CdSe QDs valence band (VB) are indicated as (5) and (6) processes, respectively. The (1), (2), and (6) processes are useful in QDSSCs operation. In contrast, the remaining processes cause a reduction in QDSSCs' performance.

d.   Shortage of binding agents between QDs and TiO_2 membrane

Among QDSSCs, which are prepared based on TiO_2, the membrane is soaked directly into TOP organic solvents, where CdSe QDs are dissolved. The solvents, however, create unsustainable chemical bonding with TiO_2 molecules. Consequently, it reduces the carrier transport efficiency in QDSSCs.
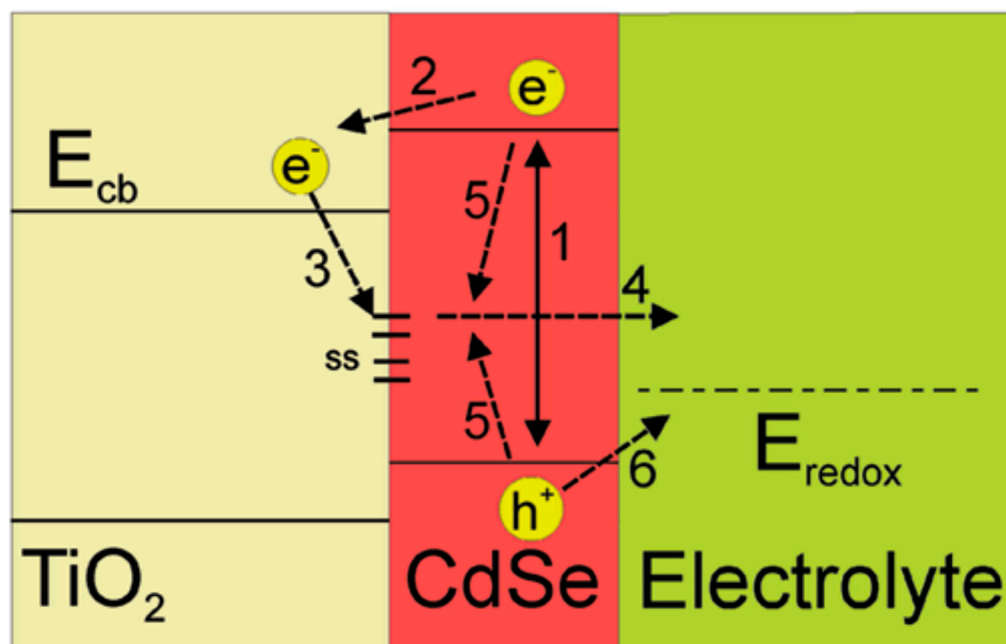
Figure 3. Schematic of the energy levels of different material layers and main processes in an operating QDSSC: (1) exciton generation in CdSe QDs, (2) electrons transferring from CdSe QDs into TiO$_2$ layer, (3) electron trapping causing by QDs' surface trap states, (4) electrons diffusion from CdSe QDs into electrolyte, (5) relaxation in CdSe QDs, and (6) recombination of electrons in electrolyte and holes in CdSe QDs by reduction reaction at the QDs/electrolyte interface. It was obtained from Mora-Sero and co-works, 2009 [79].

3. QDSSCs Based on Photoanode Binding Agents

The single QDs presented in the last section are directly absorbed onto the metal oxide membrane. It is difficult to achieve perfect absorption at the QDs/TiO$_2$ interface, hence electronic trap states have consequently arisen. To reduce the recombination at QDs/metal oxide interface, binding agents, such as mercaptopropionic acid (MPA), trioctylphosphine, or trioctylphosphine oxide [82,83], thiolacetid acid (TAA), or mercaptohexadecanoic acid [84], are frequently used. With the formation of COOH-R-SH, the COOH- (carboxyl) group of binding agents can establish chemical bonding with metal oxides, while -SH (thiol) group is linked to single QDs, as illustrated in Figure 4. The presence of binding agents supports the electron transport from the CB of QDs into the metal oxide layer, consequently, the current density enhancement in QDSSCs has been observed.
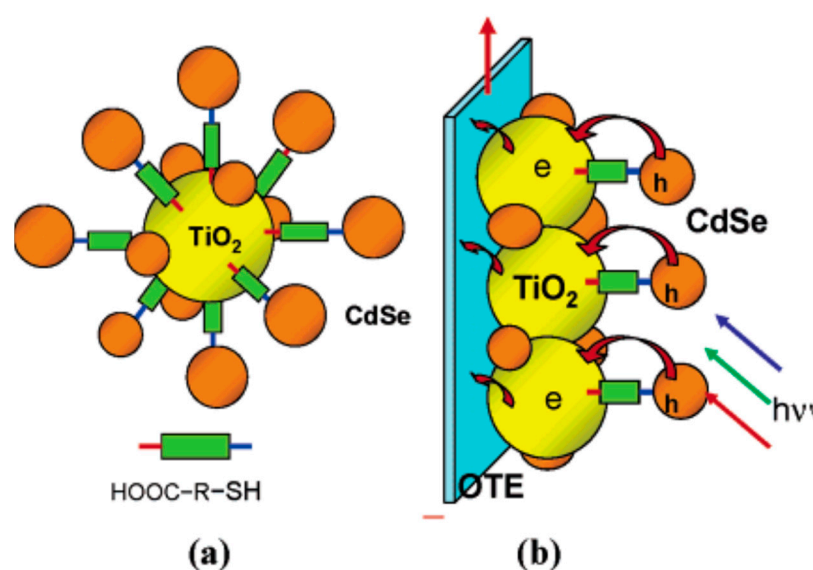
Figure 4. (**a**) The absorption of single CdSe QDs onto the metal oxide membrane supported by binding agents and (**b**) photoanode is formed by coating system (**a**) with the FTO glass substrate [84].

4. QDSSCs Based on a Photoanode with a Passive Surfactant

The actual PCE of the majority of QDSSCs, which have a single QDs photoanode, is less than from the theoretical calculation due to the strong recombination inside QDs and at QDs/TiO_2 interface or direct contact of QDs with the different electrolyte systems. To limit the number of surface trap states, materials with large band gaps, such as ZnS, SiO_2, MgO, or Al_2O_3 (shown in Table 3), have been frequently used as a passivation layer [85–90]. The passivation layer is covered on the surface of QDs to create a boundary that prevents the direct contact of QDs with the electrolyte and hence the dark current, i.e., stimulated electron transport from QDs to the electrolyte. One can imagine that the excited electrons are blocked by the presence of this passivation layer and only able to move from QDs to TiO_2 and then to the outer circuit.

Table 3. Review on QDSSCs with passive surfactant.

QDs	Passivation Layer	PCE (%)	References
CdSe	ZnS	2.1	[91]
CdS/CdSe	ZnS	4.92	[92]
$CdSe_xTe_{1-x}$	ZnS/SiO_2	8.55	[93]
PbS/CdS	ZnS	4.2	[94]
PbS/CdS	ZnS/SiO_2	7.19	[95]
CdTe/CdSe	ZnS	6.76	[96]
ZnTe/CdSe	ZnS	6.82	[97]
CdS/CdSe	ZnS	2.07	[98]
CdS/CdSe:Mn	ZnS	3.77	[99]
CdS/CdSe:Cu	ZnS	4.22	[100]

Currently, ZnS has been widely used as the most effective passive surfactant for QDSSCs since this semiconductor has a large band gap of approximately 3.6 eV and CB level (−3.6 eV) of nanocrystal ZnS is higher than that of CdSe (−4.3 eV) and CdS (−4.11 eV), which is studied by Tung et al. and illustrated in Figure 5a. The efficiency was significantly increased by 150% with the presence of a passivation layer. In addition, Tung and colleagues reported an efficiency enhancement from 1.64% to 3.77% on QDSSCs based CdS/CdSe:Mn photoanode and from 1.64% to 4.22% on CdS/CdSe:Cu-based photoanode with the presence of ZnS passivation layer [99–102]. As reported by Hachiya et al. [95], a significant improvement of excited electron transport from QDs into TiO_2 layer and

a dramatic reduction of surface trap states at the QDs/TiO_2 interface by covering ZnS nanocrystals on PbS QDs were observed and proved by transient grating (TG) spectra. Apart from ZnS, other materials, such as ZnSe [103], Al_2O_3 [104], or SiO_2 [101], have been used as a passivation layer for QDSSCs. According to Tung et al., the QDSSCs efficiency was sharply increased by 375% when a SiO_2 passivation layer was absorbed onto the surface of CdS/CdSe QDs. Since SiO_2 conduction level in a vacuum (4.5 eV) was much higher than those of CdSe (−4.3 eV) and CdS (−4.11 eV), the dark current was mostly suppressed in QDSSCs leading to the PCE enhancement. Furthermore, the combination of ZnS and SiO_2 as a passivation layer has shown promising efficiency in recent studies. The passivation layer of ZnS/SiO_2 covered on the surface of $CdSe_xTe_{1−x}$ QDs, in particular, leads to the significantly increased efficiency from 6.37% to 8.55% [103].
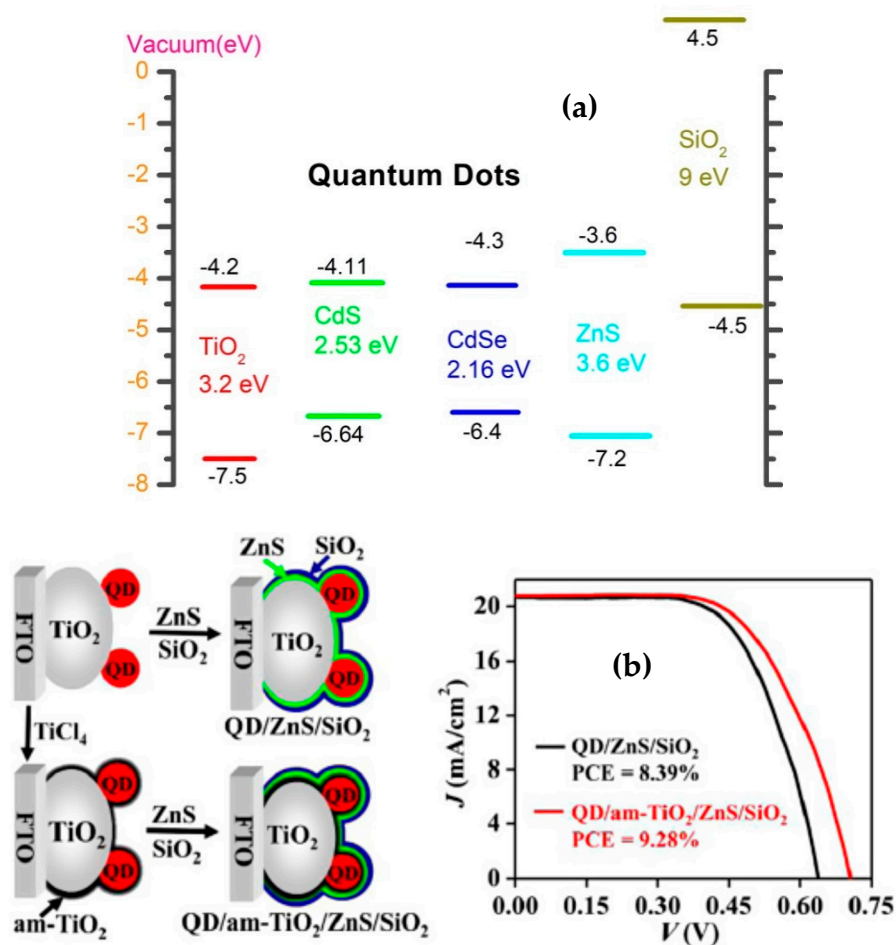

Figure 5. (**a**) Schematic diagram of the energy level of an QDSSC's photoanode [101] and (**b**) the enhancement in QDSSCs performance by using a passive surfactant from Ren and co-work, 2015 [105].

5. QDSSCs Based on a Photoanode with Multilayer QDs

QDSSCs based on single QDs have limited absorption spectra in the visible region. To overcome CdS, CdSe, CdTe, and PbS QDs are combined to be able to absorb photons with different wavelengths in the visible region. Recently, photoanodes with multilayer QDs, such as CdS/CdSe [105], CdS/CdTe [106], CdS/PbS [107], CdS/CdSe/PbS [108], CdSe/CdTe [109], or ZnTe/CdSe [110], have been studied. Osada et al. reported a 70% increasement in PCE of QDSSCs by covering a CdS layer prior to TiO_2, i.e., CdS acts as a buffer layer, while only 50% enhancement with CdSe prior covering. This result has good agreement with others reported by Tung and colleagues [111]. Specifically, they observed a raise from 0.6% to 1.05% in QDSSC' PCE when a CdS layer is sandwiched between TiO_2 and CdSe outer layers. Several publications on the electric transport researched inside

QDSSCs based on TG spectra have proved that the tandem (or parallel or cophotosensitive) structure, as can be seen in Figure 5a, leads to more photon absorption and hence more exciton generation [112,113].

In Figure 6a, TiO_2, CdS, and CdSe are in bulk scale, so the CB level of bulk CdSe is lower than those of bulk TiO_2 and CdS. This structure obstructs the electron movement from the CB of CdS and CdSe QDs into the TiO_2 layer. However, when CdS and CdSe are in the nanoscale, their band gap can be manipulated. As can be seen in Figure 6b, the band gaps of CdS and CdSe nanocrystals were 2.39 and 1.8 eV, respectively. Due to quantum confinement, the conduction energy levels of both CdS and CdSe nanocrystals were higher than that of bulk TiO_2. This yielded a tandem structure at the photoanode energy, which is favorable for electron transport from QDs into TiO_2. Moreover, with the tandem structure shown in Figure 6, light propagates in order through FTO, TiO_2, CdS, CdSe, and ZnS layers. FTO glass substrate is transparent, so light energy is preserved when reaching the TiO_2 layer. Due to the large bandgap of 3.2 eV, the TiO_2 layer just absorbed photons with wavelengths less than 400 nm. Other longer wavelength photons were continuously propagated and then those with wavelengths less than 450 nm and 650 nm were absorbed by CdS and CdSe QDs, respectively. Therefore, the tandem structure of photoanode energy led to a broader absorption spectrum from the ultraviolet region to 650 nm in the visible region and more exciton generation, consequently, PCE of QDSSCs may be enhanced. However, the excited electrons can be trapped by a number of surface states at TiO_2/CdS/CdSe/ZnS interface due to the imperfect synthesis process, which affects the performance of QDSSCs [100].
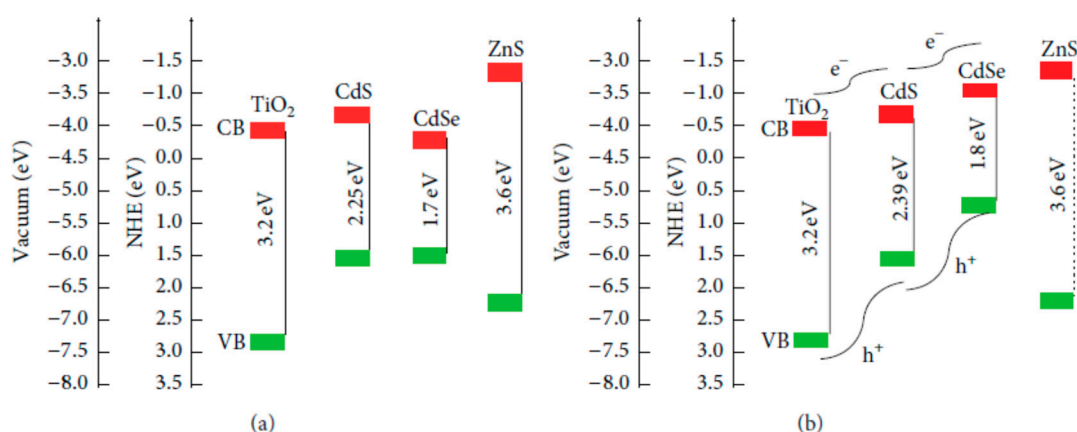

Figure 6. Schematic diagram of the energy level of a photoanode with (**a**) CdS CdSe in bulk scale and (**b**) CdS CdSe in the nanoscale from Grätzel, 2001 [114].

6. QDSSCs Based on a Photoanode with Doped QDs

In recent years, CdSe QDs has been attractively researched and applied in QDSSCs fabrication due to their simple synthesis, low cost, and high chemical stability. The resistance, however, of CdSe was relatively high and the CB level of this material in the bulk state was slightly slower than that of TiO_2, which obstructed the movement of photoexcited electrons from the CB of CdSe QDs into TiO_2. To improve the current density and hence the PCE of QDSSCs, several research have been carried out on doping metals, such as Mg [115], Mn [99], Cu [100], Ag [116], Hg [117], Co [118], or Eu [119], into CdS, CdSe or PbS QDs.

As reported by Tung et al., by doping Mn and Cu into CdSe QDs, the efficiencies of QDSSCs were increased from 2.55% with pure tandem-structure photoanode to 3.77% and 4.22% with Mn- and Cu-doped photoanode, respectively. These results have good agreement with those in Reference [97]. The current density enhancement in QDSSCs with the doped photoanode was due to the presence of doping metal energy level in the bandgap of pure QDs, as can be seen in Figure 7b. Hence, one can manipulate the

bandgap of QDs, for instance, CdSe:Cu^{2+} QDs, by controlling the doping concentration and layer thickness. Without doping, photons whose energy was less than the pure QDs bandgap cannot be absorbed. However, by the presence of doping energy levels inside the pure QDs bandgap, those aforementioned photons were able to be absorbed. This led to a significant improvement of the photoexcited electron density and hence the current density of QDSSCs [120–122]. Moreover, by doping metals into pure QDs, the resistance of different components in QDSSCs, such as TiO_2/QDs interface and TiO_2 diffusion layer resistance (R_{ct2}) or electrolyte/counter electrode resistance (R_{ct1}), were dramatically decreased, while the significant increasement of photoexcited electron lifetime in the QDs CB was observed [100].
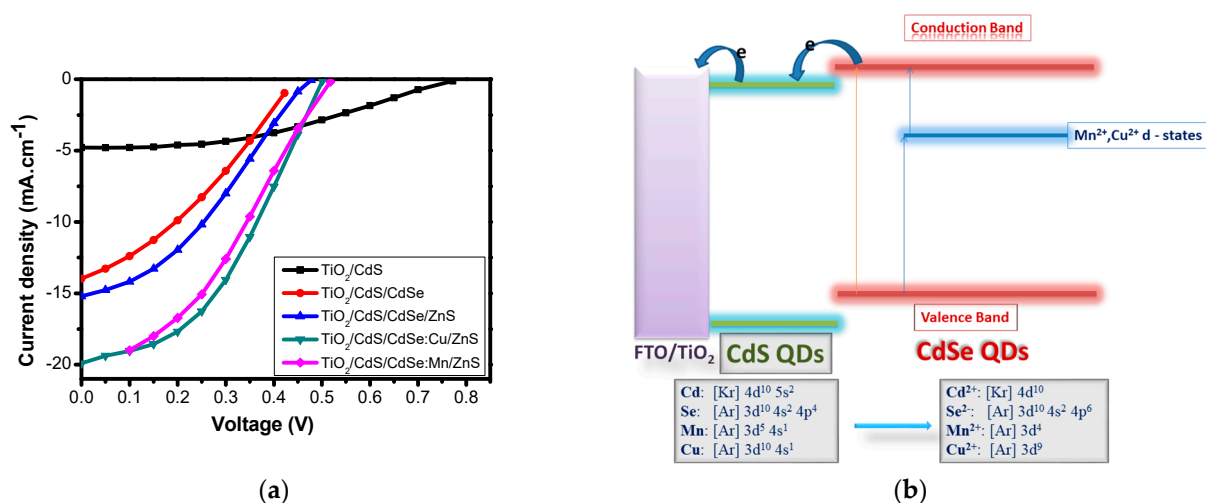

Figure 7. (**a**) Current density–voltage (J–V) curves of QDSSCs with different photoanodes and (**b**) schematic diagram of the energy level of a photoanode with CdSe QDs doped Mn or Cu from Phuc, D.H and co-works, 2019 [120].

7. QDSSCs Based on Different Counter Electrodes

Counter electrode has a large contribution on the operation of QDSSCs, so choosing the suitable material for counter electrode fabrication is strongly required. The reduction reaction of the electrolyte system is occurred at the counter electrode surface, hence the counter electrode material must have low resistance and high electrochemical catalyst activity, i.e., to reduce the redox potential of the electrolyte. Pt was previously used as the cathode material due to its compatibility with the I^{3-}/I^- electrolyte as a Figure 9. However, the resistance of the counter electrode/electrolyte interface is relatively high, which reduces the electron transport efficiency through the cathode surface [123]. For QDSSCs, QDs are easily corroded in the I^{3-}/I^- electrolyte and hence limit the light absorption ability of those QDs. Several cathode materials, such as nanocarbon tubes, CuS, nanocarbon tube–Cu_2S, NiS, or Au (Figures 8 and 9) [124–126], have been studied in QDSSCs with a polysulfide electrolyte. Among them, nanocarbon tube, Au and NiS are suitable for the polysulfide electrolyte but have high resistance at the counter electrode/electrolyte interface, hence limiting the electron movement from counter electrode to electrolyte and reduce the efficiency of QDSSCs. CoS and NiS materials have been studied for better results, but they leave impurities in the electrolyte and counter electrode, which affect QDSSCS in the long-term operation [127,128].
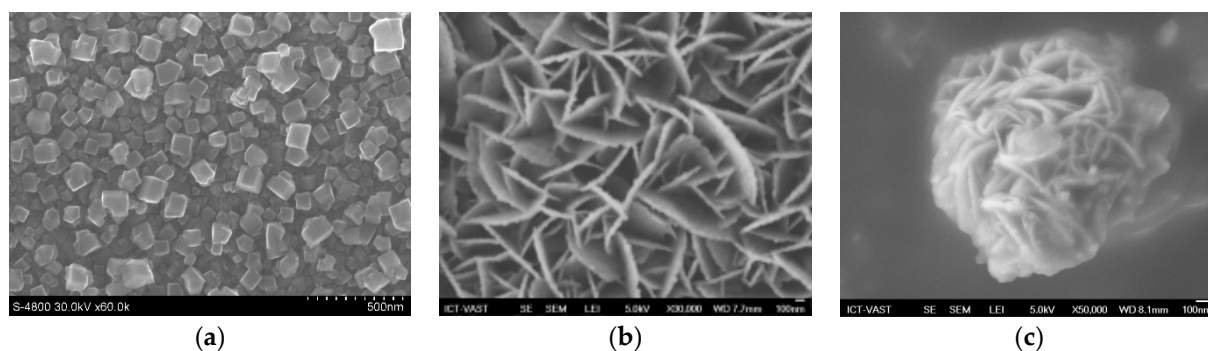
Figure 8. FE-SEM images of counter electrodes based on different materials: (**a**) PbS, (**b**) CuS, and (**c**) Cu_2S from Tung HT and co-works, 2014 [129].
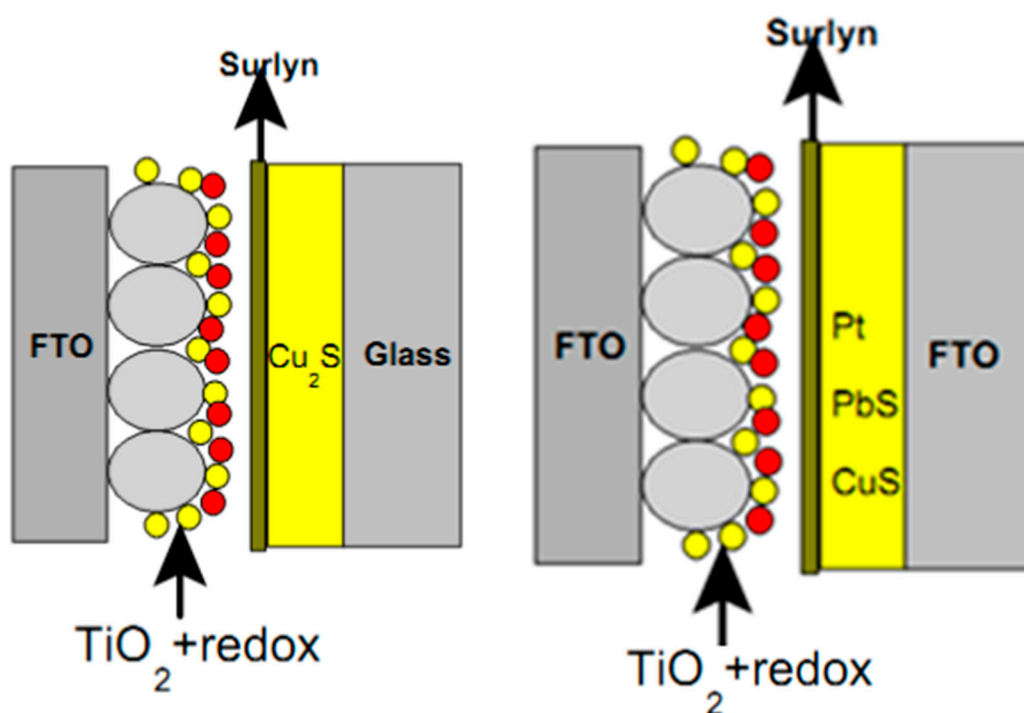

Figure 9. Schematic diagram of QDSSCs' structure with different counter electrode materials: Cu_2S (**left**) and Pt, CuS, and PbS (**right**).

Graphene is a two-dimensional single layer of carbon atoms, which has a large surface area and high electronic mobility of 1.5×10^4 cm^2 V^{-1} s^{-1} so having prominent electrical, optical, thermal dynamics, and mechanical properties [130–132]. Therefore, graphene has become promising for science and technology revolution. Moreover, graphene oxide is more applicable due to possessing -COOH and -OH function groups lying between horizontal lattices and on the corner of the horizontal plane, which can form carbonyl or carboxylic (Figure 10) to easily establish chemical bonding with inorganic materials, such as Cu_xS, on counter electrodes of QDSSCs.
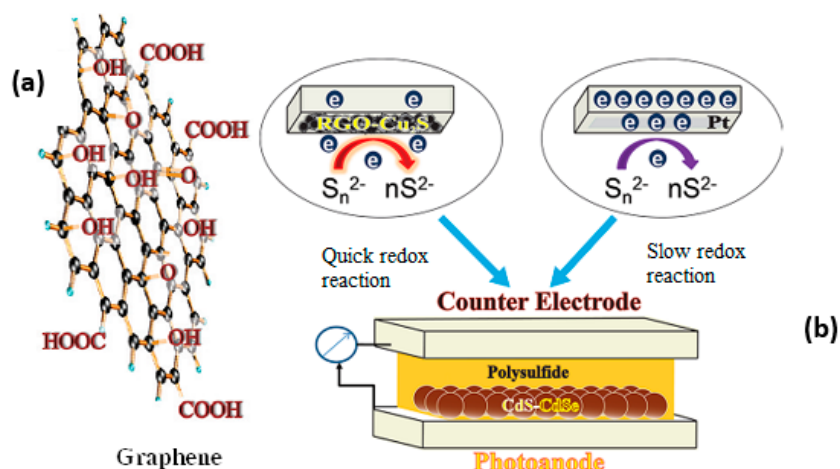
Figure 10. (**a**) Graphene with functional groups and (**b**) structure of a QDSSC from Tachan and co-works, 2011 [133].

Cu_xS and its compounds have superior absorption and decompose chemical reaction ability, which lead to efficiency enhancement, so they have been widely used as counter electrode materials in QDSSCs [134]. Lee et al. studied the composite of Cu_2S and nanocarbon tube, but only 0.08% efficiency was achieved due to the carrier mobility of the nanocarbon tube is much lower than that of graphene [135].

8. QDSSCs Based on Different Electrolytes

As discussed in Section 6, QDSSCs derived from the previous type of solar cells, which had dye molecules as photo absorbers, so keep using the I^-/I^{3-} electrolyte. This electrolyte, however, is the main cause of corrosion and functional degradation of QDs and hence low efficiency, for instance, 1.52% PCE of QDSSCs based on CdS/CdSe QDs [123]. Therefore, seeking for a more compatible electrolyte with QDs to improve QDSSCs performance is the main challenge. The electrolyte, according to recent reports (Table 4), can now be divided into three categories, which are liquid, pseudo-solid, and solid electrolytes.

Table 4. Review on QDSSCS based on different counter electrodes.

Counter Electrode	QDs	PCE (%)	References
Pt	CdS/CdSe	1.52	[123]
Au	CdS/CdSe	4.22	[136]
Cu_xS	$CdSe_xTe_{1-x}$	9.28	[137]
Cu_xS	$CdSe_xTe_{1-x}$	8.72	[138]
Cu_2S	$CdSe_xTe_{1-x}$	6.12	[139]
CoS	CdS/CdSe	4.16	[140]
Cu_2S	CdS/CdSe:Cu	4.22	[100]
rGO-Cu_2S	CdS/CdSe	4.4	[141]
NiS	CdS	2.5	[142]
NiS_2	CdS/CdSe	2.25	[143]
PbS	CdS/CdSe	3.91	[144]

Among them, liquid polysulfide electrolyte has been widely used due to its compatibility with QDs and counter electrodes, which greatly improve the QDSSCS performance [144]. This electrolyte, unfortunately, causes oxidation of the QDs and makes the open circuit potential (V_{OC}) and FF low [145]. To protect from corrosion, QDs are frequently covered by a layer of passivation surfactants, such as ZnS or SiO_2, as discussed above. In addition to the polysulfide electrolyte, the pseudo-solid [146] or solid [147] electrolyte has been used in

the combination with organic compounds, such as polyethylene glycol [148] and guanidine thiocyanate [149].

9. Opportunities and Challenges

Currently, QDs have been made with high purity, quality, less defects, manipulated bandgap energy, and good optical properties to replace photosensitive molecules. However, the PCE of QCSSCs has not exceeded 10%, which is much lower than that from theoretical calculations. There are two major issues one has to overcome:

Firstly, substantial excitation electron loss in QDSSCs. There are many types of losses in QDSSCs operation, such as the recombination process inside QDs or on their surfaces due to imperfect fabrication, electron loss when transported through the QDs/TiO$_2$ interface, electron diffusion process inside the TiO$_2$ membrane, and QDs corrosion by electrolyte or electron loss due to redox reaction at the electrolyte/counter electrode interface. Among them, the losses due to internal and surface defects of QDs are limited for those QDs synthesized by the colloidal process at high temperature or extended for those made by the CBD or SILAR method. Losses due to electrolyte corrosion can be improved by using passivation surfactants, such as ZnS or SiO$_2$, to limit the contact between QDs and electrolytes. However, more defects are observed in the multilayer photoanodes with tandem structure.

Secondly, researching on the new kind of QDs materials.

a. QDSSCs based on QDs possessing intermediate band (IB)

Limitations in traditional solar cells, such as a narrow absorption spectrum of photosensitive materials, leads to the degradation of absorbed photon density, current density, and open circuit potential. Those photons, which have energy larger or equal than the photosensitive material bandgap, are absorbed. For materials with IB structure, this issue is overcome since the material is a compound of two or more materials with different bandgap energies. As can be seen in Figure 11, photons with different energies E$_1$, E2, and E$_3$ are absorbed, corresponding to the energy gap between two VBs of the two materials, valence and CBs of the narrower bandgap material and two CBs of the two materials, respectively. These absorptions result in the enhancement of the excited electron concentration in the CB of a wider bandgap material, which is then collected and transferred to an external circuit and creates the electric current density. These IB structure materials have great potential to replace traditional photosensitive materials due to predicted PCE in QDSSCs up to 46% [150].
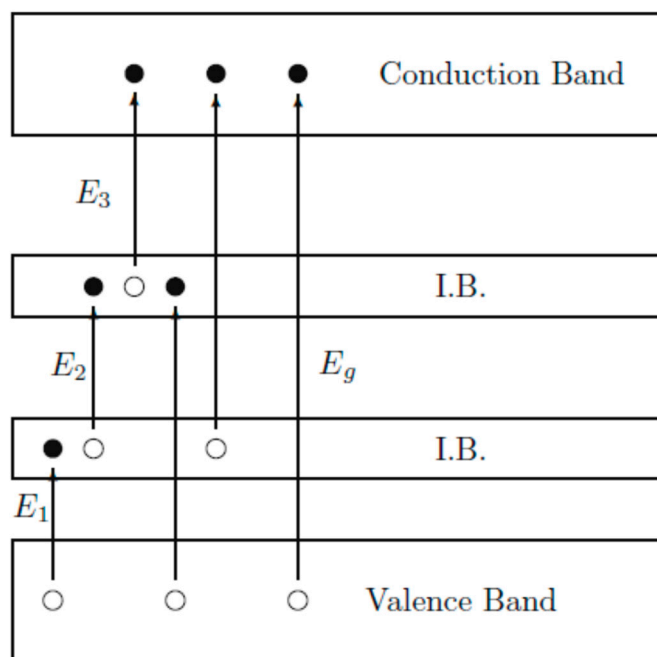
Figure 11. Schematic diagram of energy levels of an IB structure material from Wu and co-works, 2012 [151].

b.   Graphene thin film with QDs for photoanode fabrication

Graphene is a two-dimensional single layer of carbon atoms, which has a large surface area and high electronic mobility of 1.5×10^4 cm^2 V^{-1} s^{-1} so having prominent electrical, optical, thermal dynamics, and mechanical properties [151–153]. Carbon-based graphene materials have outstanding properties, especially graphene quantum dots with extremely effective electron transport properties, and other interesting phenomena due to the quantum confinement effect [154]. Therefore, graphene has become promising for science and technology revolution. Several reports on this kind of material have been observed. Dutta et al. synthesized graphene QDs and then absorbed onto the surface of ZnO fibers by chemical deposition method, resulting in a 0.8 V open circuit potential [154]. Zhong and colleagues combined graphene QDs with CdSe QDs covering the TiO$_2$ membrane for 6% conversion efficiency [155]. Graphene QDs combined with other QDs, such as CdSe, CdS, or CdTe, is an effective method to improve PCE of QDSSCs.

Figure 12 shows a schematic diagram of a QDSSCs based on a photoanode with graphene. Core–shell structure CdSe/ZnS QDs absorbed on a graphene membrane has demonstrated the faster electron transportation from QDs to the TiO$_2$ layer [156]. The superiority of graphene is demonstrated in another report, which studied the transient absorption spectrum of pure and CdTe QDs absorbed graphene resulting in a significant increase of relaxation time from 50 ps in pure QDs to 200 ps in absorbed graphene and hence increases the excitation electron density in the CB of QDs and is the basis for increasing the current density in QDSSCs [157].
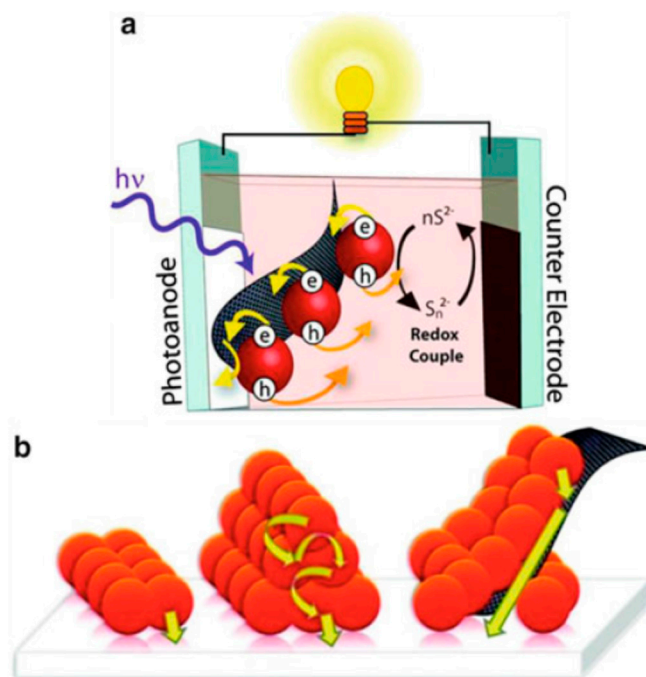
Figure 12. (**a**) Structure of QDSSCs based on graphene/CdSe QDs photoanode and (**b**) schematic of a photoanode that has graphene/CdSe QDs absorbing on the FTO substrate.

Author Contributions: N.T.K.C.: Formal analysis; funding acquisition; investigation, writingreview & editing. P.T.N.: Formal analysis; writingreview & editing. H.T.T.: Conceptualization; data curation; formal analysis; funding acquisition; investigation; methodology; writing-original draft; writingreview & editing. D.H.P.: Conceptualization; data curation; formal analysis; funding acquisition; investigation; methodology; writing-original draft; writing-review & editing. All authors have read and agreed to the published version of the manuscript.

Conflicts of Interest: The authors declare no conflict of interest.

References

1. Yoshikawa, K.; Kawasaki, H.; Yoshida, W.; Irie, T.; Konishi, K.; Nakano, K.; Uto, T.; Adachi, D.; Kanematsu, M.; Uzu, H.; et al. Silicon heterojunction solar cell with interdigitated back contacts for a photoconversion efficiency over 26%. *Nat. Energy* **2017**, *2*, 1–8. [CrossRef]
2. Richter, A.; Benick, J.; Feldmann, F.; Fell, A.; Hermle, M.; Glunz, S.W. n-Type Si solar cells with passivating electron contact: Identifying sources for efficiency limitations by wafer thickness and resistivity variation. *Sol. Energy Mater. Sol. Cells* **2017**, *173*, 96–105. [CrossRef]
3. Wang, T.; Ren, S.; Li, C.; Li, W.; Liu, C.; Zhang, J.; Wu, L.; Li, B. Exploring window buffer layer technology to enhance CdTe solar cell performance Back contact Window layer 40 nm. *Sol. Energy* **2018**, *164*, 180–186. [CrossRef]
4. Ichikawa, Y.; Yoshida, T.; Hama, T.; Sakai, H.; Harashima, K. Production technology for amorphous silicon-based # exible solar cells. *Sol. Energy Mater. Sol. Cells* **2001**, *66*, 107–115.
5. Kato, T.; Handa, A.; Yagioka, T.; Matsuura, T.; Yamamoto, K.; Higashi, S. Enhanced Efficiency of Cd-Free Cu (In, Ga)(Se, S)2 Minimodule Via (Zn, Mg) O Second Buffer Layer and Alkali Metal Post-Treatment. *IEEE J. Photovolt.* **2017**, *7*, 1173–1180. [CrossRef]
6. Yang, W.S.; Noh, J.H.; Jeon, N.J.; Kim, Y.C.; Ryu, S.; Seo, J.; Seok, S.I. Highperformance photovoltaic perovskite layers fabricated through intramolecular exchange. *Science* **2015**, *348*, 1234–1237. [CrossRef]
7. Stolterfoht, M.; Grischek, M.; Caprioglio, P.; Wolff, C.M.; Gutierrez-Partida, E.; Peña-Camargo, F.; Rothhardt, D.; Zhang, S.; Raoufi, M.; Wolansky, J.; et al. How to Quantify the Efficiency Potential of Neat Perovskite Films: Perovskite Semiconductors with an Implied Efficiency Exceeding 28%. *Adv. Mater.* **2020**, *32*, 2000080. [CrossRef]
8. Nozik, A.J. Quantum Dot Solar Cells. *Physica E* **2002**, *14*, 115–120. [CrossRef]
9. Green, M.A.; Emery, K.; Hishikawa, Y.; Warta, W. Improved optical transmission and current matching of a triple-junction solar cell utilizing sub-wavelength structures. *Prog. Photovolt.* **2009**, *17*, 320–326. [CrossRef]

10. Graetzel, M.; Janssen, R.A.J.; Mitzi, D.B.; Sargent, E.H. Materials interface engineering for solution processed photovoltaics. *Nature* **2012**, *488*, 304–312. [CrossRef]

11. Kinoshita, T.; Dy, J.T.; Uchida, S.; Kubo, T.; Segawa, H. Wideband dye-sensitized solar cells employing a phosphine-coordinated ruthenium sensitizer. *Nat. Photonics* **2013**, *7*, 535–539. [CrossRef]

12. Kim, J.Y.; Voznyy, O.; Zhitomirsky, D.; Sargent, E.H. Colloidal quantum dot materials and devices: A quarter-century of advances. *Adv. Mater.* **2015**, *25*, 4986–5010. [CrossRef] [PubMed]

13. Tian, J.; Zhang, Q.; Uchaker, E.; Gao, R.; Qu, X.; Zhang, S.; Cao, G. ZnO/TiO₂ nanocable structured photoelectrodes for CdS/CdSe quantum dot co-sensitized solar cells. *Energy Environ. Sci.* **2013**, *6*, 3542. [CrossRef]

14. Phuc, D.H.; Tung, H.T. Quantum dot sensitized solar cell based on the different photoelectrodes for the enhanced performance. *Sol. Energy Mater. Sol. Cells* **2019**, *196*, 78–83.

15. Tung, H.T.; Phuc, D.H.; Chung, N.T.K.; Thuy, N.T.N. Enhanced light absorption and charge recombination control in quantum dot sensitized solar cells using Copper and Manganese doped cadmium sulfide quantum dots. *Environ. Prog. Sustain. Energy* **2021**, e13650. [CrossRef]

16. Thanh, T.H.; Vinh, L.Q.; Dat, H.T. The Dynamic Resistance of CdS/CdSe/ZnS Co-Sensitized TiO₂ Solar Cells. *Braz. J. Phys.* **2014**, *44*, 746–752. [CrossRef]

17. Phuc, D.H.; Tung, H.T. The effect of thickness on the performance of CdSe: Cu 2+—quantum dot-sensitized solar cells. *Appl. Phys.* **2018**, *11*, 1–9.

18. Li, T.L.; Lee, Y.L.; Teng, H. High-performance quantum dot-sensitized solar cells based on sensitization withCuInS₂ quantum dots/CdS heterostructure. *Energy Environ. Sci.* **2012**, *5*, 5315–5324. [CrossRef]

19. Sugaya, T.; Numakami, O.; Oshima, R.; Furue, S.; Komaki, H.; Amano, T.; Matsubara, K.; Okano, Y.; Niki, S. Type II GaSb quantum ring solar cells under concentrated sunlight. *Energy Environ. Sci.* **2012**, *5*, 6233–6237. [CrossRef]

20. Kamat, P.V. Quantum Dot Solar Cells. Semiconductor Nanocrystals as Light Harvesters. *J. Phys. Chem. C* **2008**, *112*, 18737–18753. [CrossRef]

21. Kamat, P.V. Quantum Dot Solar Cells. The Next Big Thing in Photovoltaics. *J. Phys. Chem. Lett.* **2013**, *4*, 908–918. [CrossRef] [PubMed]

22. Farahani, F.A.; Poro, A.; Rezaee, M.; Sameni, M. Enhancement in power conversion efficiency of CdS quantum dot sensitized solar cells through a decrease in light reflection. *Opt. Mater.* **2020**, *108*, 110248. [CrossRef]

23. Tyagi, J.; Gupta, H.; Purohit, L.P. Cascade Structured ZnO/TiO₂/CdS quantum dot sensitized solar cell. *Solid State Sci.* **2020**, *102*, 106176. [CrossRef]

24. Tian, J.J.; Zhang, Q.F.; Zhang, L.L.; Gao, R.; Shen, L.F.; Zhang, S.G.; Qu, X.H.; Cao, G.Z. Architectured ZnO photoelectrode for high efficiency quantum dot sensitized solar cells. *Nanoscale* **2013**, *5*, 936–943. [CrossRef]

25. Hossain, M.A.; Jennings, J.R.; Koh, Z.Y.; Wang, Q. CdSe-sensitized mesoscopic TiO₂ solar cells exhibiting >5% efficiency: Redundancy of CdS buffer layer. *ACS Nano* **2011**, *5*, 3172–3181. [CrossRef]

26. Ganguly, A.; Nath, S.S.; Srivastava, V.M. Enhanced efficiency in swift 100 mev ni ion irradiated zns quantum dot sensitized solar cell. *Chalcogenide Lett.* **2020**, *17*, 487–493.

27. Marandi, M.; Abadi, S.H. Aqueous synthesis of colloidal CdSeₓTe₁₋ₓ–CdS core–shell nanocrystals and effect of shell formation parameters on the efficiency of corresponding quantum dot sensitized solar cells. *Sol. Energy* **2020**, *209*, 387–399. [CrossRef]

28. Deng, J.; Li, L.; Gou, Y.; Fang, J.; Feng, R.; Lei, Y.; Song, X.; Yang, Z. CdS-derived CdS₁₋ₓSeₓ nanocrystals within TiO₂ films for quantum dot-sensitized solar cells prepared through hydrothermal anion exchange reaction. *Electrochim. Acta* **2020**, *356*, 136845. [CrossRef]

29. Robel, I.; Kuno, M.; Kamat, P.V. Size-dependent electron injection from excited CdSe quantum dots into TiO₂ nanoparticles. *J. Am. Chem. Soc.* **2007**, *129*, 4136–4137. [CrossRef]

30. Yu, W.W.; Peng, X.G. Formation of high-quality CdS and other II–VI semiconductor nanocrystals in noncoordinating solvents: Tunable reactivity of monomers. *Angew. Chem. Int. Ed.* **2002**, *41*, 2368–2371.

31. Vogel, R.; Pohl, K.; Weller, H. Sensitization of highly porous, polycrystalline TiO₂ electrodes by quantum sized CdS. *Chem. Phys. Lett.* **1990**, *174*, 241–246. [CrossRef]

32. Lee, H.-J.; Kim, D.-Y.; Yoo, J.-S.; Bang, J.; Kim, S.; Park, S.-M. Anchoring cadmium chalcogenide quantum dots (QD) onto stable oxide semiconductor for QD sensitized solar cells. *Bull. Kor. Chem. Soc.* **2008**, *28*, 953–958.

33. Lee, H.-J.; Yum, J.-H.; Leventis, H.C.; Zakeeruddin, S.M.; Haque, S.A.; Chen, P.; Seok, S.I.; Gratzel, M.; Nazeeruddin, M.-K. CdSe quantum dot-sensitized solar cells exceeding efficiency 1% at full sun intensity. *J. Phys. Chem. C* **2008**, *112*, 11600–11608. [CrossRef]

34. Lee, W.J.; Kang, S.H.; Min, S.-K.; Sung, Y.-E.; Han, S.-H. Co-sensitization of vertically aligned TiO₂ nanotubes with two different sizes of CdSe quantum dots for broad spectrum. *Electrochem. Commun.* **2008**, *10*, 1579–1582. [CrossRef]

35. Kim, J.Y.; Lee, K.; Coates, N.E.; Moses, D.; Nguyen, T.Q.; Dante, M.; Heeger, A.J. Efficient tandem polymer solar cells fabricated by all solution processing. *Science* **2007**, *317*, 222–225. [CrossRef] [PubMed]

36. Yu, P.R.; Zhu, K.; Norman, A.G.; Ferrere, S.; Frank, A.J.; Nozik, A.J. Nanocrystalline TiO₂ solar cells sensitized with InAs quantum dots. *J. Phys. Chem. B* **2006**, *50*, 25451–25454.

37. Giménez, S.; Iván, M.-S.; Lorena, M.; Nestor, G.; Teresa, L.-V.; Roberto, G.; Diguna, L.J.; Shen, Q.; Toyoda, T.; Bisquert, J. Improving the performance of colloidal quantum-dot-sensitized solar cells. *Nanotechnology* **2009**, *29*, 295204. [CrossRef]

38. Diguna, L.J.; Shen, Q.; Kobayashi, J.; Toyoda, T. High efficiency of CdSe quantum-dot-sensitized TiO$_2$ inverse opal solar cells. *Appl. Phys. Lett.* **2007**, *91*, 023116.

39. Tachibana, Y.; Umekita, K.; Otsuka, Y.; Kuwabata, S. Performance improvement of CdS quantum dots sensitized TiO$_2$ solar cells by introducing a dense TiO$_2$ blocking layer. *J. Phys. D Appl. Phys.* **2008**, *41*, 102002. [CrossRef]

40. Cheng, S.; Fu, W.; Yang, H.; Zhang, L.; Ma, J.; Zhao, H.; Sun, M.; Yang, L. Photoelectrochemical performance ofmultiple semiconductors (CdS/CdSe/ZnS) cosensitized TiO$_2$ photoelectrodes. *J. Phys. Chem. C* **2012**, *116*, 2615–2621. [CrossRef]

41. Chen, L.C.; Ho, Y.C.; Yang, R.Y.; Chen, J.H.; Huang, C.M. Electrode posited AgInSe$_2$ onto TiO$_2$ films for semiconductor- sensitized solar cell application: The influence of electrode posited time. *J. Appl. Surf. Sci.* **2012**, *58*, 6558–6563. [CrossRef]

42. Huazheng, L.; Lu, W.; Song, B.; Zhou, J.; Zhao, G.; Han, G. The design of Mn^{2+} & Co^{2+} co-doped CdTe quantum dot sensitized solar cells with much higher efficiency. *RSC Adv.* **2020**, *10*, 35701–35708.

43. Dongho, L.; Choi, W.; Yang, J. Investigation of the Trap-Induced Power Conversion Limit for CdS/CdSe Cascade Quantum Dot Sensitized Solar Cells Fabricated by Using the Successive Ionic Layer Adsorption and Reaction Process. *J. Korean Phys. Soc.* **2020**, *76*, 1133–1143.

44. Mahmoud, S.; Dehghani, M.; Parand, P.; Najafi, M.N.; Parvazian, E. Photovoltaic performance and electrochemical impedance spectroscopy analysis of CdS/CdSe-sensitized solar cell based on surfactant-modified ZnS treatment. *Appl. Phys. A* **2020**, *126*, 1–8.

45. Huashang, R.; Zhou, M.; Pan, Z.; Zhong, X. Quantum dot materials engineering boosting the quantum dot sensitized solar cell efficiency over 13%. *J. Mater. Chem. A* **2020**, *8*, 10233–10241.

46. Yunlong, D.; Lu, S.; Xu, Z.; Zhang, J.; Ma, F.; Peng, S. Enhanced performance of CdS/CdSe quantum dot-sensitized solar cells by long-persistence phosphors structural layer. *Sci. China Mater.* **2020**, *63*, 516–523.

47. Nideep, T.K.; Ramya, M.; Kailasnath, M. An investigation on the photovoltaic performance of quantum dot solar cells sensitized by CdTe, CdSe and CdS having comparable size. *Superlattices Microstruct.* **2020**, *141*, 106477. [CrossRef]

48. Elibol, E. Quantum dot sensitized solar cell design with surface passivized CdSeTe QDs. *Sol. Energy* **2020**, *206*, 741–750. [CrossRef]

49. Chakrapani, V.; Baker, D.; Kamat, P.V. Understanding the Role of the Sulfide Redox Couple (S^{2-}/Sn^{2-}) in Quantum Dot-Sensitized Solar Cells. *J. Am. Chem. Soc.* **2011**, *133*, 9607–9615. [CrossRef] [PubMed]

50. Ganguly, A.; Nath, S.S. Mn-doped CdS quantum dots as sensitizers in solar cells. *Mater. Sci. Eng. B* **2020**, *255*, 114532. [CrossRef]

51. Vadim, F.L. *Impedance Spectroscopy Applications to Electrochemical and Dielectric Phenomena*; John Wiley & Sons: Hoboken, NJ, USA, 2012.

52. Archana, T.; Vijayakumar, K.; Subashini, G.; Grace, A.N.; Arivanandhan, M.; Jayavel, R. Facile synthesis of CdS Quantum dots for QDSSC with high photo current density. *Mater. Res. Express* **2020**, *7*, 015528. [CrossRef]

53. Beaulac, R.; Archer, P.I.; Ochsenbein, S.T.; Gamelin, D.R. Mn^{2+}-Doped CdSe Quantum Dots: New Inorganic Materials for Spin-Electronics and Spin-Photonics. *Adv. Funct. Mater.* **2008**, *18*, 3873–3891. [CrossRef]

54. Karan, N.S.; Sarma, D.D.; Kadam, R.M.; Pradhan, N. Doping transition metal (Mn or Cu) ions in semiconductor nanocrystals. *J. Phys. Chem. Lett.* **2010**, *1*, 2863–2866. [CrossRef]

55. Victoria, G.P.; Sima, C.; Marzari, G.; Boix, P.P.; Giménez, S.; Shen, Q.; Dittrich, T.; Mora-Seró, I. High performance PbS Quantum Dot Sensitized Solar Cells exceeding 4% efficiency: The role of metal precursors in the electron injection and charge separation. *Phys. Chem. Chem. Phys.* **2013**, *15*, 13835–13843.

56. Santra, P.K.; Kamat, P.V. Mn-doped quantum dot sensitized solar cells: A strategy to boost efficiency over 5%. *J. Am. Chem. Soc.* **2012**, *134*, 2508–2511. [CrossRef] [PubMed]

57. Zhu, G.; Pan, L.; Xu, T.; Sun, Z. CdS/CdSe-Cosensitized TiO$_2$ Photoanode for Quantum-Dot-Sensitized Solar Cells by a Microwave-Assisted Chemical Bath Deposition Method. *ACS Appl. Mater. Interfaces* **2011**, *3*, 3146–3151. [CrossRef]

58. Lee, Y.H.; Im, S.H.; Chang, J.A.; Lee, J.H.; Seok, S.I. CdSe-sensitized inorganic-organic heterojunction solar cells: The effect of molecular dipole interface modification and surface passivation. *Org. Electron.* **2012**, *13*, 975–979. [CrossRef]

59. Maryam, O.; Dehghani, H. Improving the photovoltaic performance of CdSe$_{0.2}$S$_{0.8}$ alloyed quantum dot sensitized solar cells using CdMnSe outer quantum dot. *Sol. Energy* **2020**, *199*, 901–910.

60. Pan, Z.; Zhao, K.; Wang, J.; Zhang, H.; Feng, Y.; Zhong, X. Near infrared absorption of CdSe$_x$Te$_{1-x}$ alloyed quantum dot sensitized solar cells with more than 6% efficiency and high stability. *ACS Nano* **2013**, *7*, 5215–5222. [CrossRef]

61. Radich, J.G.; Peeples, N.R.; Santra, P.K.; Kamat, P.V. Charge transfer mediation through Cu$_x$S. The hole story of CdSe in polysulfide. *J. Phys. Chem. C* **2014**, *118*, 16463–16471. [CrossRef]

62. Wang, J.S.; Shen, Q.; Mora-Sero, I.; Wang, J.; Pan, Z.X.; Zhao, K.; Kuga, Y.; Zhong, X.H.; Bisquert, J. Band engineering in core/shell ZnTe/CdSe for photovoltage and efficiency enhancement in exciplex quantum dot sensitized solar cells. *ACS Nano* **2015**, *9*, 908–915.

63. Liu, D.; Kamat, P.V. Photoelectrochemical behaviour of thin CdSe and coupled TiO$_2$/CdSe semiconductor films. *J. Phys. Chem.* **1993**, *97*, 10769–10773. [CrossRef]

64. Fang, J.; Wu, J.; Lu, X.; Shen, Y.; Lu, Z. Sensitization of nanocrystalline TiO$_2$ electrode with quantum sized CdSe and ZnT$_c$P$_c$ molecules. *Chem. Phys. Lett.* **1997**, *270*, 145–151.

65. Peter, L.M.; Riley, D.J.; Tull, E.Z.; Wijayantha, K.G.U. Photosensitization of nanocrystalline TiO$_2$ by self-assembled layers of CdS quantum dots. *Chem. Commun.* **2002**, *10*, 1030–1031. [CrossRef]

66. Lee, W.; Kwak, W.-C.; Min, S.K.; Lee, J.-C.; Chae, W.-S.; Sung, Y.-M.; Han, S.-H. Spectral broadening in quantum dots-sensitized photoelectrochemical solar cells based on CdSe and Mg-doped CdSe nanocrystals. *Electrochem. Commun.* **2008**, *10*, 1699–1702.

67. Kongkanand, A.; Tvrdy, K.; Takechi, K.; Kuno, M.; Kamat, P.V. Quantum dot solar cells. Tuning photoresponse through size and shape control of CdSe-TiO₂ architecture. *J. Am. Chem. Soc.* **2008**, *130*, 4007–4015. [CrossRef] [PubMed]

68. Lopez-Luke, T.; Wolcott, A.; Xu, L.-P.; Chen, S.; Wen, Z.; Li, J.; Rosa, E.D.L.; Zhang, J.Z. Nitrogen-doped and CdSe quantum-dot-sensitized nanocrystalline TiO₂ films for solar energy conversion applications. *J. Phys. Chem. C* **2008**, *112*, 1282–1292. [CrossRef]

69. Mora-Sero, I.; Gimenez, S.; Moehl, T.; Fabregat-Santiago, F.; Lana-Villareal, T.; Gomez, R.; Bisquert, J. Factors determining the photovoltaic performance of a CdSe quantum dot sensitized solar cell: The role of the linker molecule and of the counter electrode. *Nanotechnology* **2008**, *19*, 424007. [CrossRef]

70. Shen, Y.-J.; Lee, Y.-L. Assembly of CdS quantum dots onto mesoscopic TiO₂ films for quantum dot-sensitized solar cell application. *Nanotechnology* **2008**, *19*, 045602. [CrossRef]

71. Chen, J.; Zhao, D.W.; Song, J.L.; Sun, X.W.; Deng, W.Q.; Liu, X.W.; Lei, W. Directly assembled CdSe quantum dots on TiO₂ in aqueous solution by adjusting pH value for quantum dot sensitized solar cells. *Electrochem. Commun.* **2009**, *11*, 2265–2267. [CrossRef]

72. Yu, X.-Y.; Lei, B.-X.; Kuang, D.-B.; Su, C.-Y. High performance and reduced charge recombination of CdSe/CdS quantum dot-sensitized solar cells. *J. Mater. Chem.* **2012**, *22*, 12058–12063. [CrossRef]

73. Jung, S.W.; Park, J.-H.; Lee, W.; Kim, J.-H.; Kim, H.; Choi, C.-J.; Ahn., K.-S. Enhanced electron lifetime in CdS quantum dot-sensitized solar cells with nanoporous-layer-covered TiO₂ nanotube arrays. *J. Appl. Phys.* **2011**, *110*, 054301. [CrossRef]

74. Jiao, J.; Zhou, Z.; Zhou, W.; Wu, S. CdS and PbS quantum dots co sensitized TiO₂ nanorod arrays with improved performance for solar cells. *Appl. Mater. Sci. Semicond Process* **2013**, *16*, 435–440. [CrossRef]

75. Hu, X.; Zhang, Q.; Huang, X.; Li, D.; Luo, Y.; Meng, Q. Aqueous colloidal CuInS₂ for quantum dot sensitized solar cells. *J. Mater. Chem.* **2011**, *21*, 15903. [CrossRef]

76. Veerathangam, K.; Pandian, M.S.; Ramasamy, P. Photovoltaic performance of Pb-doped CdS quantum dots for solar cell application. *Mater. Lett.* **2018**, *220*, 74–77. [CrossRef]

77. Nikolaos, B.; Vassilios, D.; Kyriakos, B.; Panagiotis, L. Quantum dot sensitized solar cells based on an optimized combination of ZnS, CdS and CdSe with CoS and CuS counter electrodes. *Electrochim. Acta* **2013**, *91*, 246–252.

78. Hodes, G.; Manassen, J.; Cahen, D. Electrocatalytic electrodes for the polysulfide redox system. *J. Electrochem. Soc.* **1980**, *127*, 544. [CrossRef]

79. Mora-Seró, I.; Bisquert, J. Breakthroughs in the development of semiconductor-sensitized solar cells. *J. Phys. Chem. Lett.* **2010**, *1*, 3046–3052. [CrossRef]

80. Senthamilselvi, V.; Saravanakumar, K.; Begum, N.J.; Anandhi, R.; Ravichandran, A.T.; Sakthivel, B. Photovoltaic properties of nanocrystalline CdS films deposited by SILAR and CBD techniques—A comparative study. *J. Mater. Sci. Mater. Electron.* **2012**, *23*, 302–308. [CrossRef]

81. Vasiliev, R.B.; Dorofeev, S.G.; Dirin, D.N.; Belov, D.A.; Kuznetsova, T.A. Synthesis and optical properties of PbSe and CdSe colloidal quantum dots capped with oleic acid. *Mendeleev Commun.* **2004**, *14*, 169–171. [CrossRef]

82. Chen, M.X.; Bai, Y.Q.; Guan, X.N.; Chen, J.W.; Zeng, J.H. Phosphating passivation layer for quantum dot sensitized solar cells. *Thin Solid Films.* **2021**, 138678. [CrossRef]

83. Guijarro, N.; Lana-Villarreal, T.; Mora-Sero, I.; Bisquert, J.; Gómez, R. CdSe quantum dot-sensitized TiO₂ electrodes: Effect of quantum dot coverage and mode of attachment. *J. Phys. Chem. C* **2009**, *113*, 4208–4214. [CrossRef]

84. István, R.; Subramanian, V.; Kuno, M.; Kamat, P.V. Quantum dot solar cells. Harvesting light energy with CdSe nanocrystals molecularly linked to mesoscopic TiO₂ films. *J. Am. Chem. Soc.* **2006**, *128*, 2385–2393.

85. Yang, S.M.; Huang, C.H.; Zhai, J.; Wang, Z.S.; Jiang, L. High photostability and quantum yield of nanoporous TiO₂ thin film electrodes Co-sensitized with capped sulfides. *J. Mater. Chem.* **2002**, *12*, 1459–1464. [CrossRef]

86. Vaishanav, S.K.; Jyoti, K.; Nagwanshi, R.; Karbhal, I.; Dewangan, L.; Ghosh, K.K.; Satnami, M.L. Interaction of Folic Acid with Mn²⁺ Doped CdTe/ZnS Quantum Dots: In Situ Detection of Folic Acid. *J. Fluoresc.* **2021**, 1–10. [CrossRef]

87. Shen, Q.; Kobayashi, J.; Diguna, L.J.; Toyoda, T. Effect of ZnS coating on the photovoltaic properties of CdSe quantum dot-sensitized solar cells. *J. Appl. Phys.* **2008**, *103*, 084304. [CrossRef]

88. Tachan, Z.; Hod, I.; Shalom, M.; Grinis, L.; Zaban, A. The importance of the TiO₂/quantum dots interface in the recombination processes of quantum dot sensitized solar cells. *Phys. Chem. Chem. Phys.* **2013**, *15*, 3841–3845. [CrossRef] [PubMed]

89. Liu, Z.; Miyauchi, M.; Uemura, Y.; Cui, Y.; Hara, K.; Zhao, Z.; Sunahara, K.; Furube, A. Enhancing the performance of quantum dots sensitized solar cell by SiO2 surface coating. *Appl. Phys. Lett.* **2010**, *96*, 233107. [CrossRef]

90. Brennan, T.P.; Trejo, O.; Roelofs, K.E.; Xu, J.; Prinz, F.B.; Bent, S.F. Efficiency enhancement of solid-state PbS quantum dot-sensitized solar cells with Al₂O₃ barrier layer. *J. Mater. Chem. A* **2013**, *1*, 7566–7571. [CrossRef]

91. Grätzel, M. Mesoscopic Solar Cells for Electricity and Hydrogen Production from Sunlight. *Chem. Lett.* **2005**, *34*, 8–13. [CrossRef]

92. Zhang, Q.; Guo, X.; Huang, X.; Huang, S.; Li, D.; Luo, Y.; Shen, Q.; Toyoda, T.; Meng, Q. Highly efficient CdS/CdSe-sensitized solar cells controlled by the structural properties of compact porous TiO2 photoelectrodes. *Phys. Chem. Chem. Phys.* **2011**, *13*, 4659–4667. [CrossRef]

93. Zhao, K.; Pan, Z.; Mora-Seró, I.; Cánovas, E.; Wang, H.; Song, Y.; Gong, X.; Wang, J.; Bonn, M.; Bisquert, J.; et al. Boosting Power Conversion Efficiencies of Quantum-Dot-Sensitized Solar Cells Beyond 8% by Recombination Control. *J. Am. Chem. Soc.* **2015**, *137*, 5602–5609. [CrossRef]

94. Simi, N.J.; Bernadsha, S.B.; Thomas, A.; Ison, V.V. Quantum Dot Sensitized Solar Cells using Type-II CdSe-Cu₂Se Core-Shell QDs. *Results Opt.* **2021**, 100088. [CrossRef]

95. Jiao, S.; Wang, J.; Shen, Q.; Li, Y.; Zhong, X. Surface engineering of PbS quantum dot sensitized solar cells with a conversion efficiency exceeding 7%. *J. Mater. Chem. A* **2016**, *4*, 7214–7221. [CrossRef]

96. Wang, J.; Mora-Seró, I.; Pan, Z.; Zhao, K.; Zhang, H.; Feng, Y.; Yang, G.; Zhong, X.; Bisquert, J. Core/Shell Colloidal Quantum Dot Exciplex States for the Development of Highly Efficient Quantum-Dot-Sensitized Solar Cells. *J. Am. Chem. Soc.* **2013**, *135*, 15913–15922. [CrossRef] [PubMed]

97. Choudhury, B.D.; Lin, C.; Shawon, S.M.Z.; Soliz-Martinez, A.J.; Huq, H.; Uddin, M.J. A photoanode with hierarchical nanoforest TiO₂ structure and silver plasmonic nanoparticles for flexible dye sensitized solar cell. *Sci. Rep.* **2011**, *11*, 1–11.

98. Thanh, T.H.; Quang, V.L.; Thanh, D.H. Determination of the dynamic resistance of the quantum dots solar cells by one I–V curve and electrochemical impedance spectra. *Sol. Energy Mater. Sol. Cells* **2015**, *143*, 269–274. [CrossRef]

99. Thu, T.N.; Phuong, H.N.; Tung, H.T.; Phat, N.T.; Dat, H.T.; Vinh, L.Q. The enhanced current density of the quantum dots solar cells based on CdSe: Mn2+ crystalline. *Opt. Mater.* **2018**, *84*, 199–204. [CrossRef]

100. Nguyen, T.P.; Ha, T.T.; Nguyen, T.T.; Ho, N.P.; Huynh, T.D.; Lam, Q.V. Effect of Cu²⁺ ions doped on the photovoltaic features of CdSe quantum dot sensitized solar cells. *Electrochim. Acta* **2018**, *282*, 16–23. [CrossRef]

101. Tung, H.T.; Thao, N.T.; Vinh, L.Q. The Reduced Recombination and the Enhanced Lifetime of Excited Electron in QDSSCs Based on Different ZnS and SiO2 Passivation. *Int. J. Photoenergy* **2018**, *2018*, 1–8. [CrossRef]

102. Ren, Z.W.; Wang, Z.Q.; Wang, R.Q.; Pan, Z.X.; Gong, X.Q.; Zhong, X.H. Effects of metal oxyhydroxide coatings on photoanode in quantum dot sensitized solar cells. *Chem. Mater.* **2016**, *28*, 2323–2330. [CrossRef]

103. Ning, Z.; Tian, H.; Yuan, C.; Fu, Y.; Qin, H.; Sun, L.; Ågren, H. Solar cells sensitized with type-II ZnSe-CdS core/shell colloidal quantum dots. *Chem. Commun.* **2011**, *47*, 1536–1538. [CrossRef]

104. Roelofs, K.E.; Brennan, T.P.; Dominguez, J.C.; Bailie, C.D.; Margulis, G.Y.; Hoke, E.T.; McGehee, M.D.; Bent, S.F. Effect of Al₂O₃ Recombination Barrier Layers Deposited by Atomic Layer Deposition in Solid-State CdS Quantum Dot-Sensitized Solar Cells. *J. Phys. Chem. C* **2013**, *117*, 5584–5592. [CrossRef]

105. Ren, Z.; Wang, J.; Pan, Z.; Zhao, K.; Zhang, H.; Li, Y.; Zhao, Y.; Mora-Sero, I.; Bisquert, J.; Zhong, X. Amorphous TiO₂ buffer layer boosts efficiency of quantum dot sensitized solar cells to over 9%. *Chem. Mater.* **2015**, *27*, 8398–8405. [CrossRef]

106. Chuang, C.-H.M.; Brown, P.R.; Bulović, V.; Bawendi, M.G. Improved performance and stability in quantum dot solar cells through band alignment engineering. *Nat. Mater.* **2014**, *13*, 796–801. [CrossRef]

107. Cao, Y.; Stavrinadis, A.; Lasanta, T.; So, D.; Konstantatos, G. The role of surface passivation for efficient and photostable PbS quantum dot solar cells. *Nat. Energy* **2016**, *1*, 16035. [CrossRef]

108. Azmi, R.; Oh, S.-H.; Jang, S.-Y. High-Efficiency Colloidal Quantum Dot Photovoltaic Devices Using Chemically Modified Heterojunctions. *ACS Energy Lett.* **2016**, *1*, 100–106. [CrossRef]

109. Kim, G.-H.; De Arquer, F.P.G.; Yoon, Y.J.; Lan, X.; Liu, M.; Voznyy, O.; Jagadamma, L.K.; Abbas, A.S.; Yang, Z.; Fan, F.; et al. Correction to High-Efficiency Colloidal Quantum Dot Photovoltaics via Robust Self-Assembled Monolayers. *Nano Lett.* **2015**, *16*, 822. [CrossRef] [PubMed]

110. Lin, Z.; Franceschetti, A.; Lusk, M.T. Size Dependence of the Multiple Exciton Generation Rate in CdSe Quantum Dots. *ACS Nano* **2011**, *5*, 2503–2511. [CrossRef]

111. Thanh, T.H.; Lam, Q.V.; Nguyen, T.H.; Huynh, T.D. Performance of CdS/CdSe/ZnS quantum dot-sensitized TiO₂ mesopores for solar cells. *Chin. Opt. Lett.* **2013**, *11*, 72501–72504. [CrossRef]

112. Wang, Q.; Li, S.; Liu, P.; Min, X. Bio-templated CdSe quantum dots green synthesis in the functional protein, lysozyme, and biological activity investigation. *Mater. Chem. Phys.* **2012**, *137*, 580–585. [CrossRef]

113. Cordova, R.; Gómez, H.; Schrebler, R.; Cury, P.; Orellana, M.; Grez, P.; Leinen, D.; Ramos-Barrado, J.R.; Del Río, R. Electrosynthesis and Electrochemical Characterization of a Thin Phase of Cu_xS (x→2) on ITO Electrode. *Langmuir* **2002**, *18*, 8647–8654. [CrossRef]

114. Grätzel, M. Photoelectrochemical cells. *Nature* **2001**, *414*, 338. [CrossRef]

115. Grätzel, M. Dye-sensitized solar cells. *J. Photochem. Photobiol. C: Photochem. Rev.* **2003**, *4*, 145–153. [CrossRef]

116. Tung, H.T.; Van Thuan, D.; Kiat, J.H.; Phuc, D.H. Ag+ ion doped on the CdSe quantum dots for quantum-dot-sensitized solar cells' application. *Appl. Phys. A* **2019**, *125*, 505. [CrossRef]

117. Lee, J.W.; Son, D.Y.; Ahn, T.K.; Shin, H.W.; Kim, I.Y.; Hwang, S.J.; Ko, M.J.; Sul, S.; Han, H.; Park, N.G. Quantum-dot-sensitized solar cell with unprecedentedly high photocurrent. *Sci. Rep.* **2013**, *3*, 1050. [CrossRef] [PubMed]

118. Fan, S.-Q.; Cao, R.-J.; Xi, Y.-X.; Gao, M.; Wang, M.-D.; Kima, D.-H. CdSe quantum dots as cosensitizers of organic dyes in solar cells for red-shifted light harvesting. *Optoelectron. Adv. Mater. Rapid. Commun.* **2009**, *10*, 1027–1033.

119. Lee, Y.-L.; Huang, B.-M.; Chien, H.-T. Highly efficient CdSe-sensitized TiO₂ photoelectrode for quantum-dot-sensitized solar cell applications. *Chem. Mater.* **2008**, *20*, 6903–6905. [CrossRef]

120. Dezhkam, M.; Zakery, A.; Keshavarz, A. Intersubband, interband transitions, and optical properties of two vertically coupled hemispherical quantum dots with wetting layers. *Chin. Opt. Lett.* **2016**, *14*, 121904. [CrossRef]

121. Jung, S.W.; Kim, J.H.; Kim, H.; Choi, C.J.; Ahn, K.S. ZnS over layer on in situ chemical bath deposited CdS quantum dot assembled TiO₂ films for quantum dot-sensitized solar cells. *J. Curr. Appl. Phys.* **2012**, *12*, 1459–1464. [CrossRef]

122. Zewdu, T.; Clifford, J.N.; Hernández, J.P.; Palomares, E. Photo-induced charge transfer dynamics in efficient TiO₂/CdS/CdSe sensitized solar cells. *Energy Environ. Sci.* **2011**, *4*, 4633. [CrossRef]

123. Ha, T.T.; Chi, C.H.; Vy, N.T.; Thoa, N.T.P.; Huynh, T.D.; Lam, Q.V. Improving the performance of QDSSCs based on TiO$_2$/CdS (Silar)/CdSe(Colloid)/Zns(Silar) photoanodes. *Environ. Prog. Sustain. Energy* **2015**, *34*, 1774–1779. [CrossRef]

124. Hodes, G.; Manassen, J.; Cahen, D. Photo-electrochemical energy conversion: Electrocatalytic sulphur electrodes. *J. Appl. Electrochem.* **1977**, *7*, 181–182. [CrossRef]

125. Basit, M.A.; Abbas, M.A.; Naeem, H.M.; Ali, I.; Jang, E.; Bang, J.H.; Park, T.J. Ultrathin TiO$_2$-coated SiO$_2$ nanoparticles as light scattering centers for quantum dot-sensitized solar cells. *Mater. Res. Bull.* **2020**, *127*, 110858. [CrossRef]

126. Yu, Z.R.; Du, J.H.; Guo, S.H.; Zhang, H.Y.; Matsumoto, Y. CoS thin films prepared with modified chemical bath deposition. *Thin Solid Films* **2002**, *415*, 173–176. [CrossRef]

127. Que, M.; Guo, W.; Zhang, X.; Li, X.; Hua, Q.; Dong, L.; Pan, C. Flexible quantum dot-sensitized solar cells employing CoS nanorod arrays/graphite paper as effective counter electrodes. *J. Mater. Chem. A* **2014**, *2*, 13661. [CrossRef]

128. Lin, C.-Y.; Teng, C.Y.; Li, T.L.; Lee, Y.L.; Teng, H. Photoactive p-type PbS as a counter electrode for quantum dot-sensitized solar cells. *J. Mater. Chem. A* **2013**, *1*, 1155–1162. [CrossRef]

129. Thanh, H.T.; Thanh, D.H.; Lam, V.Q. The CdS/CdSe/ZnS Photoanode Co-sensitized Solar Cells Based on Pt, CuS, Cu$_2$S, and PbS Counter Electrodes. *Adv. Optoelectron.* **2014**, *2014*, 397681. [CrossRef]

130. Wu, Z.-S.; Feng, X.L.; Müllen, K. Graphene-metal oxide hybrids for lithium ion batteries and electrochemical capacitors. In *Nanocarbon-Inorganic Hybrids*; De Gruyter: Berlin, Germany, 2014; pp. 319–340.

131. Zhang, W.D.; Dong, F.; Xiong, T.; Zhang, Q. Synthesis of BiOBr–graphene and BiOBr–graphene oxide nanocomposites with enhanced visible light photocatalytic performance. *Ceram. Int.* **2014**, *40*, 9003–9008. [CrossRef]

132. Cai, D.Y.; Jin, J.; Yusoh, K.; Rafiq, R.; Song, M. High performance polyurethane/functionalized graphene nanocomposites with improved mechanical and thermal properties. *Compos. Sci. Technol.* **2012**, *72*, 702–707. [CrossRef]

133. Tachan, Z.; Shalom, M.; Hod, I.; Ruhle, S.; Tirosh, S.; Zaban, A. PbS as a highly catalytic counter electrode for polysulfide-based quantum dot solar cells. *J. Phys. Chem. C* **2011**, *115*, 6162–6166. [CrossRef]

134. Zhao, Y.; Pan, H.; Lou, Y.; Qiu, X.; Zhu, J.; Burda, C. Plasmonic Cu$_{2-x}$S Nanocrystals: Optical and Structural Properties of Copper-Deficient Copper(I) Sulfides. *J. Am. Chem. Soc.* **2009**, *131*, 4253–4261. [CrossRef]

135. Lee, H.; Yoon, S.W.; Kim, E.J.; Park, J. In situ growth of coppersulfide nanocrystals on multi walled carbon Nano tubes and their application as novel solar cell and amperometric glucose sensor materials. *Nano Lett.* **2007**, *7*, 778–784. [CrossRef] [PubMed]

136. Lee, Y.L.; Lo, Y.S. Highly efficient quantum-dot-sensitized solar cell based on co-sensitization of CdS/CdSe. *Adv. Funct. Mater.* **2009**, *19*, 604–609. [CrossRef]

137. Huang, P.; Xu, S.J.; Zhang, M.; Zhong, W.; Xiao, Z.X.; Luo, Y.P. Modulation doping of absorbent cotton derived carbon dots for quantum dot-sensitized solar cells. *Phys. Chem. Chem. Phys.* **2019**, *21*, 26133–26145. [CrossRef] [PubMed]

138. Zhang, H.; Wang, C.; Peng, W.X.; Yang, C.; Zhong, X.H. Quantum dot sensitized solar cells with efficiency up to 8.7% based on heavily copper-deficient copper selenide counter electrode. *Nano Energy* **2016**, *23*, 60–69. [CrossRef]

139. Jiang, Y.; Yu, B.B.; Liu, J.; Li, Z.H.; Sun, J.K.; Zhong, X.H.; Hu, J.-S.; Song, W.G.; Wan, L.-J. Boosting the open circuit voltage and fill factor of QDSSCs using hierarchically assembled ITO@ Cu$_2$S nanowire array counter electrodes. *Nano Lett.* **2015**, *15*, 3088–3095. [CrossRef] [PubMed]

140. Faber, M.S.; Park, K.; Cabán-Acevedo, M.; Santra, P.K.; Jin, S. Earth-abundant cobalt pyrite (CoS$_2$) thin film on glass as a robust, high-performance counter electrode for quantum dot-sensitized solar cells. *J. Phys. Chem. Lett.* **2013**, *4*, 1843–1849. [CrossRef] [PubMed]

141. Radich, J.G.; Dwyer, R.; Kamat, P.V. Cu$_2$S reduced graphene oxide composite for high-efficiency quantum dot solar cells. Overcoming the redox limitations of S$_2^-$/Sn^{2-} at the counter electrode. *J. Phys. Chem. Lett.* **2011**, *2*, 2453–2460. [CrossRef]

142. Han, Q.; Zheng, H.; Wu, M. Designing Metal-Sulfide-Sphere Counter-Electrode Catalysts for ZnO-Nanorod-Array-Based Quantum-Dot-Sensitized Solar Cells. *Eur. J. Inorg. Chem.* **2017**, *32*, 3787–3793. [CrossRef]

143. Yang, Y.; Zhu, L.; Sun, H.; Huang, X.; Luo, Y.; Li, D.; Meng, Q. Composite counter electrode based on nanoparticulate PbS and carbon black: Towards quantum dot-sensitized solar cells with both high efficiency and stability. *ACS Appl. Mater. Interfaces* **2012**, *4*, 6162–6168. [CrossRef]

144. Duan, J.; Zhang, H.; Tang, Q.; He, B.; Yu, L. Recent advances in critical materials for quantum dot-sensitized solar cells: A review. *J. Mater. Chem. A* **2015**, *3*, 17497–17510. [CrossRef]

145. Shen, Q.; Ayuzawa, Y.; Katayama, K.; Sawada, T.; Toyoda, T. Separation of ultrafast photoexcited electron and hole dynamics in CdSe quantum dots adsorbed onto nanostructured TiO$_2$ films. *Appl. Phys. Lett.* **2010**, *97*, 263113. [CrossRef]

146. Herzog, C.; Belaidi, A.; Ogacho, A.; Dittrich, T. Inorganic solid state solar cell with ultra-thin nanocomposite absorber based on nanoporous TiO$_2$ and In$_2$S$_3$. *Energy Environ. Sci.* **2009**, *2*, 962–964. [CrossRef]

147. Kim, H.; Hwang, I.; Yong, K. Highly durable and efficient quantum dot-sensitized solar cells based on oligomer gel electrolytes. *ACS Appl. Mater. Interfaces* **2014**, *6*, 11245. [CrossRef] [PubMed]

148. Du, J.; Meng, X.; Zhao, K.; Li, Y.; Zhong, X. Performance enhancement of quantum dot sensitized solar cells by adding electrolyte additives. *J. Mater. Chem. A* **2015**, *3*, 17091–17097. [CrossRef]

149. Chou, C.Y.; Lee, C.P.; Vittal, R.; Ho, K.C. Efficient quantum dot-sensitized solar cell with polystyrene-modified TiO$_2$ photoanode and with guanidine thiocyanate in its polysulfide electrolyte. *J. Power Sources* **2011**, *196*, 6595–6602. [CrossRef]

150. Jenks, S.; Gilmore, R. Quantum dot solar cell: Materials that produce two intermediate bands. *J. Renew. Sustain. Energy* **2010**, *2*, 13111. [CrossRef]

151. Wu, Z.-S.; Zhou, G.; Yin, L.-C.; Ren, W.; Li, F.; Cheng, H.-M. Graphene/metal oxide composite electrode materials for energy storage. *Nano Energy* **2012**, *1*, 107–131. [CrossRef]

152. Zhang, X.; Chang, X.; Gondal, M.A.; Zhang, B.; Liu, Y.; Ji, G. Synthesis and photocatalytic activity of graphene/BiOBr composites under visible light. *Appl. Surf. Sci.* **2012**, *258*, 7826–7832. [CrossRef]

153. Yadav, S.K.; Cho, J.W. Functionalized graphene nanoplatelets for enhanced mechanical and thermal properties of polyurethane nanocomposites. *Appl. Surf. Sci.* **2013**, *266*, 360–367. [CrossRef]

154. Dutta, M.; Sarkar, S.; Ghosh, T.; Basak, D. ZnO/Graphene Quantum Dot Solid-State Solar Cell. *J. Phys. Chem. C* **2012**, *116*, 20127–20131. [CrossRef]

155. Zhong, Y.; Zhang, H.; Pan, D.; Wang, L.; Zhong, X. Graphene quantum dots assisted photovoltage and efficiency enhancement in CdSe quantum dot sensitized solar cells. *J. Energy Chem.* **2015**, *24*, 722–728. [CrossRef]

156. Chen, Z.; Berciaud, S.; Nuckolls, C.; Heinz, T.F.; Brus, L.E. Energy Transfer from Individual Semiconductor Nanocrystals to Graphene. *ACS Nano* **2010**, *4*, 2964–2968. [CrossRef] [PubMed]

157. Kaniyankandy, S.; Rawalekar, S.; Ghosh, H.N. Ultrafast Charge Transfer Dynamics in Photoexcited CdTe Quantum Dot Decorated on Graphene. *J. Phys. Chem. C* **2012**, *116*, 16271–16275. [CrossRef]